

Joint Synthesis of Safety Certificate and Safe Control Policy using Constrained Reinforcement Learning

Haitong Ma

MAHT19@MAILS.TSINGHUA.EDU.CN

School of Vehicle and Mobility, Tsinghua University, Beijing 100084, China

Changliu Liu

CLIU6@ANDREW.CMU.EDU

Robotics Institute, Carnegie Mellon University, Pittsburgh, PA 15213, USA

Shengbo Eben Li

LISHBO@TSINGHUA.EDU.CN

Sifa Zheng

ZSF@TSINGHUA.EDU.CN

School of Vehicle and Mobility, Tsinghua University, Beijing 100084, China

Jianyu Chen

JIANYUCHEN@TSINGHUA.EDU.CN

Institute of Interdisciplinary Information Science, Tsinghua University, Beijing 100084, China

Abstract

Safety is the major consideration in controlling complex dynamical systems using reinforcement learning (RL), where the *safety certificate* can provide provable safety guarantee. A valid safety certificate is an energy function indicating that safe states are with low energy, and there exists a corresponding *safe control policy* that allows the energy function to always dissipate. The safety certificate and the safe control policy are closely related to each other and both challenging to synthesize. Therefore, existing learning-based studies treat either of them as prior knowledge to learn the other, which limits their applicability with general unknown dynamics. This paper proposes a novel approach that simultaneously synthesizes the energy-function-based safety certificate and learns the safe control policy with CRL. We do not rely on the prior knowledge about *either* an available model-based controller *or* a perfect safety certificate. In particular, we formulate a loss function to optimize the safety certificate parameters by minimizing the occurrence of energy increases. By adding this optimization procedure as an outer loop to the Lagrangian-based constrained reinforcement learning (CRL), we jointly update the policy and safety certificate parameters, and prove that they will converge to their respective local optima, the optimal safe policy and a valid safety certificate. We evaluate our algorithms on multiple safety-critical benchmark environments. The results show that the proposed algorithm learns provably safe policies with no constraint violation. The validity, or feasibility of synthesized safety certificate is also verified numerically.

Keywords: Safe Control, Safe Reinforcement Learning, Safety Certificate Synthesis, Energy Function

1. Introduction

Safety is critical when applying the state-of-the-art artificial intelligence studies to real-world applications, like autonomous driving (Sallab et al., 2017; Chen et al., 2021), robotic control (Richter et al., 2019; Ray et al., 2019). Safe control is the most common tasks among these real-world applications, which requires that the hard safety constraint must be obeyed persistently. Learning a safe control policy is hard for naive trial-and-error mechanism of RL, since it penalizes the dangerous action *after* experiencing it.

Meanwhile, in the control theory, there exist studies about provable *energy-function-based* safety guarantee of dynamic systems called the *safety certificate*, or *safety index* (Wieland and Allgöwer, 2007; Ames et al., 2014; Chang et al., 2020). These methods first synthesize an energy function such that the safe states are with low energy, and then design control laws satisfying the *safe action constraint* to make the system dissipate energy (Wei and Liu, 2019). If there exists feasible control for all states in a safe set to satisfy the *safe action constraint* dissipating the energy, then the system will never leave the safe set (i.e., forward invariance). Despite its soundness, the safety index synthesis (SIS) by hand is extremely hard for complicated or unknown systems, which stimulates a rapidly growing interest in learning-based SIS (Chang et al., 2020; Saveriano and Lee, 2019; Srinivasan et al., 2020; Qin et al., 2021). These studies assume to know the dynamical models (either white-box or black-box). Adding *safety shields or layers* to supervise RL policies is common for safety guarantee with energy function in RL (Wang et al., 2017; Cheng et al., 2019; Taylor et al., 2020; Ma et al., 2021a), but these studies usually assume the perfectness of safety certificates.

In general safe control tasks with unknown dynamics, one usually has access to neither the dynamics nor perfect safety certificates, which makes the previous two kinds of studies fall into a paradox—we can not assume either one to learn the other. Therefore, in this paper, we propose a novel algorithm without prior knowledge about models or safety certificates. We define a loss function for SIS by minimizing the occurrence of energy increases. Then we formulate a CRL problem (rather than the commonly used shielding methods) to unify the mathematical formulations of SIS and CRL. By adding SIS as an outer loop to the Lagrangian-based solution to CRL, we jointly update the policies and safety certificates, and prove that they will converge to their respective local optima, the optimal safe policies and the valid safety certificates.

Contributions. Our main contributions are: 1. We propose a joint algorithm of CRL and SIS that simultaneously learns the safe policies and synthesizes the safety certificates. This is the first algorithm requiring no prior knowledge of models or perfectness of the safety certificates. 2. We unify the loss function formulations of SIS and CRL. We therefore can form the multi-timescale adversarial training and prove its convergence. 3. We evaluate the proposed algorithm on multiple safety-critical benchmark environments, and demonstrate that we can simultaneously synthesize a valid safety certificate and learn a safe policy with zero constraint violation.

Related works. Safety index synthesis and safe control. Representative energy-function-based safety certificates include barrier certificates (Prajna et al., 2007), control barrier functions (CBF) (Wieland and Allgöwer, 2007), safety set algorithm (SSA) (Liu and Tomizuka, 2014) and sliding mode methods (Gracia et al., 2013). Recent learning-based studies can be mainly divided into two categories, *learning-based SIS* and *learning safe control policies supervised by certificates*. Chang et al. (2020); Luo and Ma (2021) use explicit model to rollout or compute action projections. Jin et al. (2020); Qin et al. (2021) guide certificate learning with LQR controller, Anonymous (2021) requires a black-box model to query online, and Saveriano and Lee (2019); Srinivasan et al. (2020) use labeled data to fit certificates with supervised learning. The latter one, learning safe policy with supervisory usually assumed a valid safety certificate (Wang et al., 2017; Cheng et al., 2019; Taylor et al., 2020). It’s a natural thought that one could learn the dynamical models to handle these issue (like Cheng et al., 2019), but this actually violates the original purpose of RL—no need to fully learn the models. Our work do not require dynamics or valid certificates in general complex environments with unknown dynamics.

Safety specifications in CRL. The safety specifications of conventional model-free CRL are defined by measurements on the *expectation* of states (Altman, 1999; Uchibe and Doya, 2007; Achiam

et al., 2017; Chow et al., 2017; Tessler et al., 2018; Ray et al., 2019; Stooke et al., 2020). Our previous study (see Ma et al., 2021b) proposes that safety specifications in control theory are all *state-dependent* and not consistent with ones in the previous CRL. Based on Lagrangian-based methods, our previous study adopte a neural network to approximate the state-dependant Lagrange multipliers to solve CRL with state-dependant safety specifications. Moreover, we provide a convergence analysis to the overall optimization scheme that is not included in Ma et al. (2021b).

2. Problem Formulations

We study on the Markov decision process (MDP) with deterministic dynamics (a reasonable assumption when dealing with safe control problems), defined by the tuple $(\mathcal{S}, \mathcal{A}, \mathcal{F}, r, c, \gamma, \phi)$, where \mathcal{S}, \mathcal{A} is the state and action space, $\mathcal{F} : \mathcal{S} \rightarrow \mathcal{S}$ is the unknown system dynamics, $r, c : \mathcal{S} \times \mathcal{A} \times \mathcal{S} \rightarrow \mathbb{R}$ is the reward and cost function, γ is the discounted factor, and $\phi : \mathcal{S} \rightarrow \mathbb{R}$ is the energy-function-based safety certificate, or called the *safety index*.

We consider the safety specification that the system state s should be constrained in a connected and closed set \mathcal{S}_s which is called the *safe set*. \mathcal{S}_s should be a zero-sublevel set of a safety index function $\phi_0(\cdot)$ denoted by $\mathcal{S}_s = \{s | \phi_0(s) \leq 0\}$. A safe control law with respect to a specific safety index should keep the system energy low, ($\phi \leq 0$) and dissipate the energy when the system is at high energy ($\phi > 0$). Then we can get the *safe action constraint*:

Definition 1 (Safe action constraint) For a given safety index ϕ , the safe action constraint is

$$\phi(s') < \max\{\phi(s) - \eta_D, 0\} \quad (1)$$

If there exist action $a \in \mathcal{A}$ satisfying (1) at s , or the safe action set $\mathcal{U}_s(s) = \{a | \phi(s') < \max\{\phi(s) - \eta_D, 0\}\}$ is nonempty, we say s is a *feasible state*. The set of all feasible states is denoted by $\mathcal{S}_f = \{s | \mathcal{U}_s(s) \neq \emptyset\}$.

Definition 2 (Valid safety certificate) Consider the set of states on all possible trajectories $\mathcal{S}_c = \{s | d_\gamma > 0\}$, where d_γ is the discounted visiting frequency. If the safe action set is always nonempty, $\mathcal{S}_c \subseteq \mathcal{S}_f$, we say the safety index ϕ is a **valid**, or **feasible** safety certificate.

A straightforward approach is to use the ϕ_0 as the safety certificate. However, these safe action constraints are possibly not satisfied with all state in \mathcal{S}_s , especially when the actuator saturation exists or the relative degree from the safety index function ϕ_0 to control is greater than one (i.e., $\|\frac{\partial \phi_0}{\partial u}\| = 0$). For example, if ϕ_0 measures the distance between two autonomous vehicle. It is possible that one is still distant from the other vehicle, but the collision is inevitable because the relative speed is too high and brake force is limited. In this case, \mathcal{S}_s includes inevitably unsafe states. We need to assign high energy values to these inevitably-unsafe states, for example, by linearly combining the ϕ_0 and its high-order derivatives (Liu and Tomizuka, 2014). The valid safety certificate will guarantee safety by ensuring the *forward invariance* of a subset of \mathcal{S}_s .

Lemma 3 (Forward invariance (Liu and Tomizuka, 2014)) Define the zero-sublevel set of a valid safety index ϕ as $\mathcal{S}_s^\phi = \{s | \phi(s) \leq 0\}$. If ϕ is a valid safety index and $\mathcal{S}_s^\phi \subseteq \mathcal{S}_c$, then there exists policy to guarantee the forward invariance of $\mathcal{S}_s^\phi \cap \mathcal{S}$.

We therefore can formulate the CRL problem with the safe action constraints:

$$\max_{\pi} J(\pi) = \mathbb{E}_{\tau \sim \pi} \left\{ \sum_{t=0}^{\infty} \gamma^t r_t \right\} \quad \text{s.t. } \phi(s') - \max\{\phi(s) - \eta_D, 0\} < 0, \forall s \in \mathcal{S}_c \quad (2)$$

We use the Lagrangian-based approach to solve (2). As the safe action constraint is state-dependent, we use a state-dependant Lagrange multipliers $\lambda(s)$, and the Lagrange function is¹

$$\mathcal{L}'(\pi, \lambda) = \mathbb{E}_s \left\{ -v^{\pi}(s) + \lambda(s) (\phi(s') - \max\{\phi(s) - \eta_D, 0\}) \right\} \quad (3)$$

We can solve (2) by locating the saddle point of $\mathcal{L}'(\pi, \lambda)$:

$$\max_{\lambda} \min_{\pi} \mathcal{L}'(\pi, \lambda) \quad (4)$$

3. Joint Synthesis of Safety Certificate and Safe Control Policy

This section introduces the joint synthesis of safety index and safe policy. The key idea is to convert the original SIS loss to minimize the occurrence of energy increases to a unified loss of RL and SIS. We provides theoretical basis of their equivalence.

3.1. Loss Function for Safety Index Synthesis

We construct the loss for optimizing a parameterized safety index by a measurement of the *violation of constraint* (1)

$$J(\phi) = \mathbb{E}_s \left\{ [\phi(s') - \max\{\phi(s) - \eta_D, 0\}]^+ \right\} \Big|_{\pi=\pi^*} \quad (5)$$

where $[\cdot]^+$ means projecting the values to the positive half space $[0, +\infty)$, π^* is the optimal policy (also a feasible policy when ϕ is a valid safety index) of (2), and $\cdot|_{\pi=\pi^*}$ represents the agent takes $\pi^*(s)$ to reach s' . Ideally, if ϕ_f is a valid safety index, there always exists control to satisfy (1), and $J(\phi_f) = 0$. For those imperfect ϕ , the inequality constraint in (2) may not hold for all states in \mathcal{S}_c , so we can optimize the loss to get better ϕ .

Before we further optimize the loss and learn the safe policy, the joint synthesis algorithm is tricky since we need to handle *two different optimization problems*, (3) and (5). Recent similar study integrates two optimizations by weighted sum (Qin et al., 2021) or alternative update (Luo and Ma, 2021), but their methods are more like intuitive approaches and lack solid theoretical basis.

3.2. Unified Loss Function for Joint Synthesis

In this section, we show that the statewise multiplier design in (3) can actually reformulate the projection operation in (5) to unify the loss function of (3) and (5) and neglect the non-differentiable projection.

Lemma 4 (Statewise complementary slackness condition (Ma et al., 2021b)) *For the problem (2), if the safe action set is not empty at state s , the optimal multiplier and optimal policy λ^*, π^* satisfies*

$$\lambda^*(s) = 0, \phi(s') - \max\{\phi(s) - \eta_D, 0\}|_{\pi^*} < 0, \text{ or } \lambda^*(s) > 0, \phi(s') - \max\{\phi(s) - \eta_D, 0\}|_{\pi^*} = 0 \quad (6)$$

If the safe action set is empty at state s , then $\lambda^(s) \rightarrow \infty$.*

1. This Lagrange function is not the original Lagrange function of problem (2), but equivalently transferred from the original one (see Ma et al., 2021b). Appendix xx also gives the detailed explanation.

The lemma comes from the Karush-Kuhn-Tucker (KKT) necessary condition for the problem (2). Consider the Lagrange function (3) with the additional variable ϕ to optimize,

$$\mathcal{L}'(\pi, \lambda, \phi) = \mathbb{E}_s \left\{ -v^\pi(s) + \lambda(s)(\phi(s') - \max\{\phi(s) - \eta_D, 0\}) \right\} \quad (7)$$

we have the following lemma for the relationship between the loss function of policy and certificate synthesis

Lemma 5 *We clip λ in a compact set $[0, \lambda_{\max}]$, where $\lambda_{\max} > \max_{s \in \mathcal{S}_f} \lambda^*(s)$. Then*

$$\mathcal{L}'(\pi^*, \lambda^*, \phi) = \lambda_{\max} J(\phi) + \Delta \quad (8)$$

where Δ is a constant irrelevant with ϕ .

This lemma can be understood that for feasible states $s \in \mathcal{S}_f$, both clipping and multiplying the optimal multiplier render the loss term to be zero. So both two loss term focus on the violation part $\phi(s') - \max\{\phi(s) - \eta_D, 0\}$ of those $s \notin \mathcal{S}_f$.

Theorem 6 (Unified loss for joint synthesis) *The*

$$\arg \min J(\phi) = \arg \min \mathcal{L}'(\pi^*, \lambda^*, \phi) \quad (9)$$

The proof comes from the envelope theorem (Milgrom and Segal, 2002) considering Lemma 5. Finally, we unify the loss function of updating three elements: policy π , multiplier λ , and safety index function ϕ . The optimization problem is formulated by extracting the optimal policy and multipliers in (9) :

$$\min_{\phi} \max_{\lambda} \min_{\pi} \mathcal{L}'(\pi, \lambda, \phi) \quad (10)$$

4. Practical Algorithm using Constrained Reinforcement Learning

In this section, we explain the details about the practical algorithm, including implementation details and convergence analysis.

4.1. Parameterized Safety Index

In this paper, we are specially interested in the collision avoidance safety constraint, which is the exact safety constraints in our experimental environments, Safety Gym Ray et al. (2019). The safety index function $\phi_0 = d_{\min} - d$, where d is the distance between the agent and obstacle, d_{\min} is the minimum safe distance. The safety index to synthesize is in the form of Anonymous (2021)

$$\phi(s) = \sigma + d_{\min}^n - d^n - k\dot{d} \quad (11)$$

where \dot{d} is the derivative of distance with respect to time, σ, n, k are the tunable parameters we desire to optimize in the online synthesis algorithm, and we name them as $\xi = [\sigma, n, k]$ for convenience. Notably, we use this parameterization since Anonymous (2021) provides helpful results on feasibility verification. For constraints outside the scope of collision avoidance, a general rule is to linearly combine ϕ_0 and its high-order derivatives Liu and Tomizuka (2014). The observations in Safety Gym includes Lidar, speedometer, and magnetometer, which can be used to compute d and \dot{d} from observations. Generally speaking, these information should be included in observations of MDP. Otherwise, the observation can not fully describe the situation about how dangerous the agent is with respect to the safety constraint, which no longer satisfies the Markov property.

4.2. Algorithm Details

The Lagrangian-based solution to CRL with statewise safety constraint is compatible with any existing unconstrained RL baselines, and we select the off-policy maximum entropy RL framework like soft actor-critic (Haarnoja et al., 2018). According to (3), we need to add two neural network to learn a state-action value function for safety index model $Q_\phi(s, a)$ (to approximate $\phi(s') - \max\{\phi(s) - \eta_D, 0\}$) and the multipliers $\lambda(s)$.

Algorithm 1 Soft Policy Improvement in FAC-SIS

Input: Buffer \mathcal{D} , policy parameters θ , multiplier parameters ξ , safety index parameters ζ .

- 1: Initial target network parameters and buffer
- 2: **if** gradient steps $\bmod m_\pi = 0$ **then** $\theta \leftarrow \theta - \overline{\beta_\pi} G_\theta$, $\alpha \leftarrow \alpha - \overline{\beta_\alpha} G_\alpha$
- 3: **if** gradient steps $\bmod m_\lambda = 0$ **then** $\xi \leftarrow \xi + \overline{\beta_\lambda} G_\xi$
- 4: **if** gradient steps $\bmod m_\phi = 0$ **then** $\zeta \leftarrow \zeta - \overline{\beta_\zeta} G_\zeta$

Output: w_1, w_2, θ, ξ .

4.3. Convergence Analysis

The convergence proof of a three timescale adversarial training of (10) mainly follows the multi-timescale convergence according to Theorem 2 in Chapter 6 in Borkar (2009) about multiple timescale convergence of multi-variable optimization. This procedure is also adopted by some studies to explain the convergence of RL algorithms from the perspective of stochastic optimization Bhatnagar et al. (2009); Bhatnagar and Lakshmanan (2012), especially those with Lagrangian-based methods Chow et al. (2017). The major difference is that existing studies assume the Lipschitz condition, which is too strict for the function approximation of neural networks. We incorporate the recent study on *clipped stochastic gradient descent* to further improve the generalization of this convergence proof Zhang et al. (2019). We first give some assumptions:

Assumption 1 (learning rate schedules) *The learning rate schedules, $\{\beta_\theta(k), \beta_\xi(k), \beta_\zeta(k)\}$, satisfy*

$$\sum_k \beta_\theta(k) = \sum_k \beta_\xi(k) = \sum_k \beta_\zeta(k) = \infty. \quad (12)$$

$$\sum_k \beta_\theta(k)^2, \sum_k \beta_\xi(k)^2, \sum_k \beta_\zeta(k)^2 < \infty, \quad \beta_\xi(k) = o(\beta_\theta(k)), \beta_\zeta(k) = o(\beta_\xi(k)).$$

This assumption also implies that the policy converges in the fastest timescale to a local optimum for given multiplier and safety index. Then the multiplier converges to its local optimum, which is proved to be a local saddle point together with the policy. Finally, the safety index parameters converges to its local optimum point.

Proposition 7 (Clipped gradient descent) *The actual learning rate used in Algorithm 1 is*

$$\overline{\beta_\#} := \min \left\{ \beta_\#, \frac{\beta_\#}{\|G_\#\|} \right\} \quad (13)$$

where $\# \in \{w_1, w_2, \theta, \xi, \zeta\}$ is the parameters, and $G_\#$ is the corresponding gradients.

As we add SIS with FAC, we name the proposed algorithm as FAC-SIS, the detailed algorithm is demonstrated in Algorithm 1. The detailed gradient computation is in Appendix C.1.

Assumption 2 *The state and action are sampled from compact sets.*

Assumption 3 *The neural network approximation is continuously differentiable.*

As we are to finish a safe control problem that the agent should be confined in a safe set, and the actuator has physical limits, the bounded assumption is reasonable. We use multi-layer perceptron with continuous differentiable activation functions in practical implementations (details can be found in Appendix E).

Theorem 8 *Under all the aforementioned assumptions, the sequence of policy, multiplier, and safety index parameters tuple $(\theta_k, \xi_k, \zeta_k)$ converge almost surely to a locally optimal safety index parameters and its corresponding locally optimal policy and multiplier $(\theta^*, \xi^*, \zeta^*)$ as k goes to infinity.*

Proof See Appendix C.2. ■

5. Experiments

In our experiments, we focus on the following questions:

1. How does the proposed algorithm compare with other constraint RL algorithms? Can it achieve a safe policy with zero constraint violation?
2. How does the learning-based safety index synthesis outperforms the handcrafted safety index or the original safety index in the safety performance?
3. Does the synthesized safety index allow the existence of safe control in all states the agent experienced?

To demonstrate the effectiveness of proposed online synthesis rules, we select the safe reinforcement learning benchmark environments Safety Gym Ray et al. (2019) with different task types, dangerous obstacle types and sizes. We name a specific environment by $\{\text{Obstacle type}\}-\{\text{Size}\}-\{\text{Task}\}$. We select 6 environments with different tasks and constraint objectives, which are demonstrated in Figure 1. The tasks include goal-reaching commonly used by other safety certificate algorithms, and also the Push with complex control tasks.

We compare the proposed algorithm against two types of baseline algorithms:

- CRL baselines, including TRPO-Lagrangian, PPO-Lagrangian and CPO Achiam et al. (2017); Ray et al. (2019). The cost threshold is set at zero.
- FAC with original safety index ϕ_0 and handcrafted safety index ϕ_h , where $\phi_0 = d_{min} - d$ and $\phi_h = 0.3 + d_{min}^2 - d^2 - kd$, named as *FAC with ϕ_0* and *FAC with ϕ_h* . The choice of ϕ_h is what we think is an appropriate choice according to our empirical knowledge. Details about these baseline algorithms can be found in Appendix D.2.

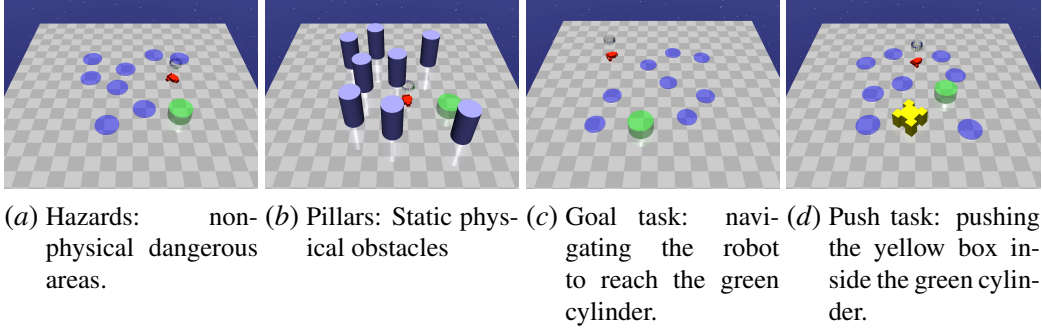


Figure 1: Obstacles and tasks in Safety Gym.

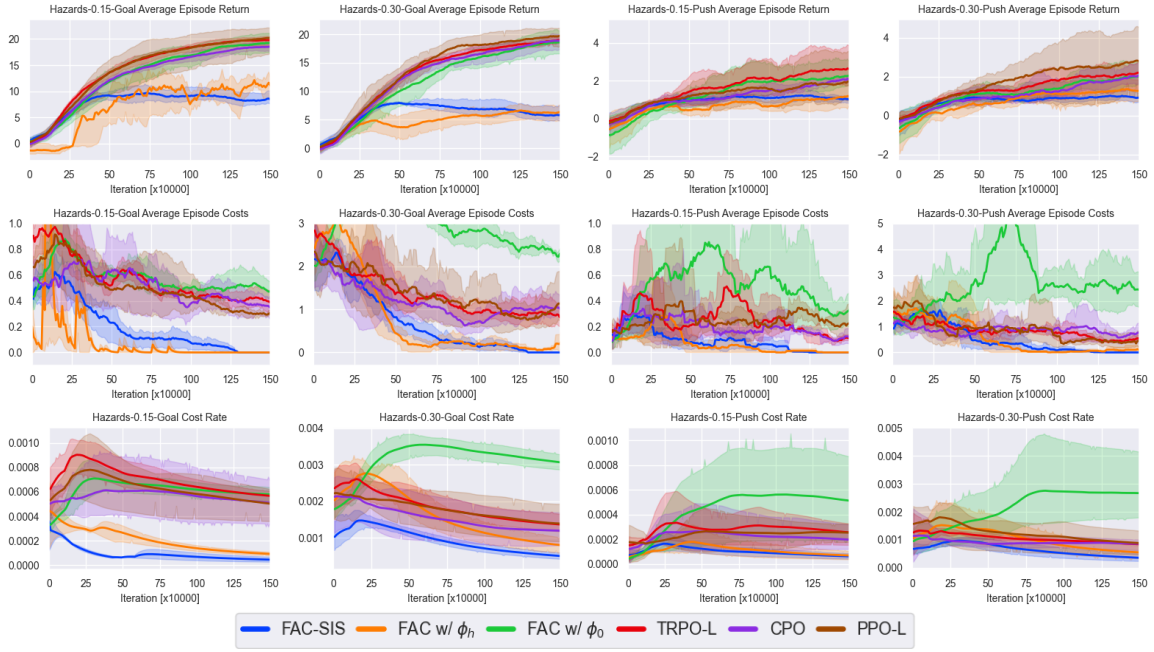


Figure 2: Average performance of FAC-SIS and baseline methods on 4 different Safety Gym environments over five seeds.

5.1. Evaluating FAC-SIS and Comparison Analysis

First, we compare the safety performance, results in 4 environments are summarized in Figure 2². The results suggest that FAC with ϕ_0 fails to provide a safe policy, and even performs poorest in the safety performance. The results reveal that there are indeed many inevitably unsafe set in \mathcal{S} , and the safety index synthesis is significant in these tasks. Only FAC-SIS learns the policy with zero violation in all environments and takes the lowest cost rate in all environments, which answers the first question that FAC-SIS provides solid safety performance. FAC with ϕ_h fails to learn a solid safe policy in those environments with 0.30 constraint size. This results show that the handcrafted

2. Others are in Appendix F.

safety index can not cover all the environments. We will explain this in detail in the next section with the feasibility analysis. The proposed FAC-SIS can adaptively fit all environments to synthesize valid safety index. As for the baseline CRL algorithms, they can not learn a zero-violation policy in any environments, and the reasons include the cost sparsity and posterior penalty for dangerous actions stated above. As for the reward performance, FAC-SIS has comparable reward performance in the `Push` task. For the `Goal` task, FAC with ϕ_h and FAC-SIS sacrifice the reward performance to guarantee safety, which is reasonable and consistent with the observations in Ray et al. (2019).

5.2. Feasibility Verification

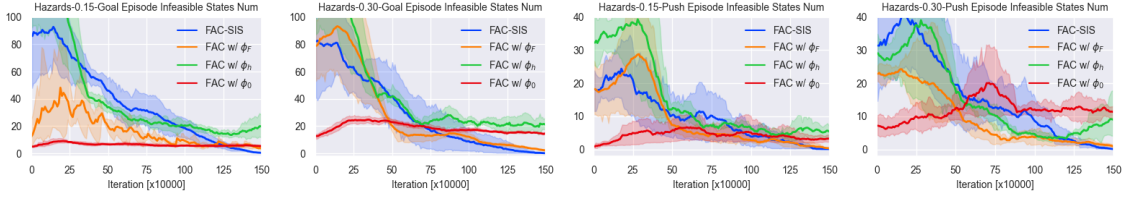


Figure 3: Average episodic number of violations of safe action constraint (1). A valid safety index and its corresponding safe control policy should have zero violation performance.

We conduct new metrics and experiments to show the feasibility of our synthesized safety index. Recall that the feasibility means that there always exists feasible control policy to satisfy the constraint in (1). To effectively demonstrate the feasibility of SIS, we add a new baseline, *FAC with ϕ_F* , where ϕ_F is a valid safety index verified by Anonymous (2021). Figure 3 demonstrates the episodic number of constraint violations of (1) in the Safety Gym environments. The results shows that FAC-SIS and *FAC with ϕ_F* can reach a nearly stable zero violation, which means that FAC can satisfy safe action constraint for a given valid safety index, and FAC-SIS also synthesizes a valid safety index. However, with ϕ_0 and ϕ_h there exists consistently violations even with the converged policy, which are caused by different reasons. For ϕ_h , the reason is rather simple for the inability to make the energy dissipate. For ϕ_0 , no high-order derivative in the safety index, so ϕ_0 cannot handle the high relative-degree between the constraint function and control input.

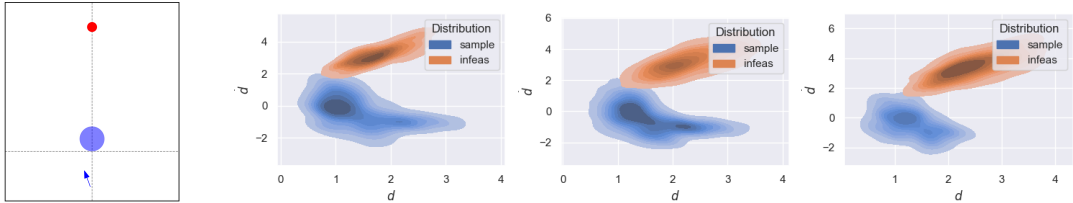


Figure 4: The custom environment and distributions of sampling state and infeasible states under three different initialization setups. The overlap of two distributions are small, which indicates that there exists feasible control for almost all sampled states.

Furthermore, we want to give a scalable analysis on how many states the agent experiences are feasible. To effectively scale the state distribution, we manually set an environment similar to the Safety Gym environments with `Point` robot, `Goal` task and `Hazard` obstacles shown in Figure 4. The agent with arrow should head to the red dot on the top while avoiding the hazard randomly located near the origin. We select 3 different initialization rules of the agent and hazard. During synthesizing the safety index with FAC-SIS, we record the state distribution in the replay buffer. Finally, we use a sample-based method to locate those infeasible states in a state set that contains the all states in the buffer distributions. First we discretize the state and action space with small interval, and we exhaust all the action to see that if the energy can dissipate for each state. If not, we remark the specific state as infeasible. For effectively illustrating these two distributions, we project the state to the 2D space of d and \dot{d} , and two state distributions on the are compared: states sampled in FAC-SIS’s buffer and infeasible states numerically verified by exhaustion, and results are listed in Figure 4. As we expect that all the sampled states should allow be feasible, these two distribution *should not overlap*. The results show that the overlap of these two distribution is very small, which indicates that nearly all the sampling states is feasible.

6. Conclusion

In this paper, we focus on joint synthesis of the safety certificate and the safe control policy for unknown dynamical system and general tasks using a CRL approach. We are the first study to start with unknown dynamics and imperfect safety certificate, which significantly improves the applicability of the energy-function-based safe control. We add the optimization of safety index parameters as an outer loop of Lagrangian-based CRL with a unified loss. The convergence to the safe control policy and the valid safety index is analyzed theoretically. Experimental results demonstrate that the proposed FAC-SIS synthesizes a valid safe index while learning a safe control policy.

In future work, we will generalize the safety index parameterization outside the scope of collision avoidance, for example, a neural network with input of features in the observation. Meanwhile, we only optimize the feasibility when formulating the loss for safety index parameters yet. We will consider other factors in SIS like the reward performance of the corresponding safe control policies.

References

- Joshua Achiam, David Held, Aviv Tamar, and Pieter Abbeel. Constrained policy optimization. In *International Conference on Machine Learning*, pages 22–31, Sydney, Australia, 2017. PMLR.
- Eitan Altman. *Constrained Markov decision processes*, volume 7. CRC Press, 1999.
- Aaron D Ames, Jessy W Grizzle, and Paulo Tabuada. Control barrier function based quadratic programs with application to adaptive cruise control. In *53rd IEEE Conference on Decision and Control*, pages 6271–6278. IEEE, 2014.
- Anonymous. Model-free safe control for zero-violation reinforcement learning. In *Submitted to 5th Annual Conference on Robot Learning*, 2021. URL <https://openreview.net/forum?id=UGp6FDaxB0f>. under review, <https://openreview.net/forum?id=UGp6FDaxB0f>.

- Shalabh Bhatnagar and K Lakshmanan. An online actor–critic algorithm with function approximation for constrained markov decision processes. *Journal of Optimization Theory and Applications*, 153(3):688–708, 2012.
- Shalabh Bhatnagar, Richard S Sutton, Mohammad Ghavamzadeh, and Mark Lee. Natural actor–critic algorithms. *Automatica*, 45(11):2471–2482, 2009.
- Vivek S Borkar. *Stochastic approximation: a dynamical systems viewpoint*, volume 48. Springer, 2009.
- Ya-Chien Chang, Nima Roohi, and Sicun Gao. Neural lyapunov control. *arXiv preprint arXiv:2005.00611*, 2020.
- Jianyu Chen, Shengbo Eben Li, and Masayoshi Tomizuka. Interpretable end-to-end urban autonomous driving with latent deep reinforcement learning. *IEEE Transactions on Intelligent Transportation Systems*, 2021.
- Richard Cheng, Gábor Orosz, Richard M Murray, and Joel W Burdick. End-to-end safe reinforcement learning through barrier functions for safety-critical continuous control tasks. In *Proceedings of the AAAI Conference on Artificial Intelligence*, volume 33, pages 3387–3395, 2019.
- Yinlam Chow, Mohammad Ghavamzadeh, Lucas Janson, and Marco Pavone. Risk-constrained reinforcement learning with percentile risk criteria. *The Journal of Machine Learning Research*, 18(1):6070–6120, 2017.
- Jingliang Duan, Yang Guan, Shengbo Eben Li, Yangang Ren, Qi Sun, and Bo Cheng. Distributional soft actor-critic: Off-policy reinforcement learning for addressing value estimation errors. *IEEE Transactions on Neural Networks and Learning Systems*, 2021.
- Luis Gracia, Fabricio Garelli, and Antonio Sala. Reactive sliding-mode algorithm for collision avoidance in robotic systems. *IEEE Transactions on Control Systems Technology*, 21(6):2391–2399, 2013.
- Tuomas Haarnoja, Aurick Zhou, Pieter Abbeel, and Sergey Levine. Soft actor-critic: Off-policy maximum entropy deep reinforcement learning with a stochastic actor. In *International Conference on Machine Learning*, pages 1861–1870, Stockholm, Sweden, 2018. PMLR.
- Wanxin Jin, Zhaoran Wang, Zhuoran Yang, and Shaoshuai Mou. Neural certificates for safe control policies. *arXiv preprint arXiv:2006.08465*, 2020.
- Changliu Liu and Masayoshi Tomizuka. Control in a safe set: Addressing safety in human-robot interactions. In *Dynamic Systems and Control Conference*, volume 46209, page V003T42A003. American Society of Mechanical Engineers, 2014.
- Yuping Luo and Tengyu Ma. Learning barrier certificates: Towards safe reinforcement learning with zero training-time violations. *arXiv preprint arXiv:2108.01846*, 2021.
- Haitong Ma, Jianyu Chen, Shengbo Eben Li, Ziyu Lin, and Sifa Zheng. Model-based constrained reinforcement learning using generalized control barrier function. *arXiv preprint arXiv:2103.01556*, 2021a.

- Haitong Ma, Yang Guan, Shegnbo Eben Li, Xiangteng Zhang, Sifa Zheng, and Jianyu Chen. Feasible actor-critic: Constrained reinforcement learning for ensuring statewise safety. *arXiv preprint arXiv:2105.10682*, 2021b.
- Paul Milgrom and Ilya Segal. Envelope theorems for arbitrary choice sets. *Econometrica*, 70(2): 583–601, 2002.
- Stephen Prajna, Ali Jadbabaie, and George J Pappas. A framework for worst-case and stochastic safety verification using barrier certificates. *IEEE Transactions on Automatic Control*, 52(8): 1415–1428, 2007.
- Zengyi Qin, Kaiqing Zhang, Yuxiao Chen, Jingkai Chen, and Chuchu Fan. Learning safe multi-agent control with decentralized neural barrier certificates. *arXiv preprint arXiv:2101.05436*, 2021.
- Alex Ray, Joshua Achiam, and Dario Amodei. Benchmarking safe exploration in deep reinforcement learning. *arXiv preprint arXiv:1910.01708*, 2019.
- Florian Richter, Ryan K Orosco, and Michael C Yip. Open-sourced reinforcement learning environments for surgical robotics. *arXiv preprint arXiv:1903.02090*, 2019.
- Ahmad EL Sallab, Mohammed Abdou, Etienne Perot, and Senthil Yogamani. Deep reinforcement learning framework for autonomous driving. *Electronic Imaging*, 2017(19):70–76, 2017.
- Matteo Saveriano and Dongheui Lee. Learning barrier functions for constrained motion planning with dynamical systems. In *2019 IEEE/RSJ International Conference on Intelligent Robots and Systems (IROS)*, pages 112–119. IEEE, 2019.
- Mohit Srinivasan, Amogh Dabholkar, Samuel Coogan, and Patricio A Vela. Synthesis of control barrier functions using a supervised machine learning approach. In *2020 IEEE/RSJ International Conference on Intelligent Robots and Systems (IROS)*, pages 7139–7145. IEEE, 2020.
- Adam Stooke, Joshua Achiam, and Pieter Abbeel. Responsive safety in reinforcement learning by pid lagrangian methods. In *International Conference on Machine Learning*, pages 9133–9143, Online, 2020. PMLR.
- Andrew Taylor, Andrew Singletary, Yisong Yue, and Aaron Ames. Learning for safety-critical control with control barrier functions. In *Learning for Dynamics and Control*, pages 708–717. PMLR, 2020.
- Chen Tessler, Daniel J Mankowitz, and Shie Mannor. Reward constrained policy optimization. *arXiv preprint arXiv:1805.11074*, 2018.
- Eiji Uchibe and Kenji Doya. Constrained reinforcement learning from intrinsic and extrinsic rewards. In *2007 IEEE 6th International Conference on Development and Learning*, pages 163–168, Lugano, Switzerland, 2007. IEEE.
- Li Wang, Aaron D Ames, and Magnus Egerstedt. Safety barrier certificates for collisions-free multirobot systems. *IEEE Transactions on Robotics*, 33(3):661–674, 2017.

Tianhao Wei and Changliu Liu. Safe control algorithms using energy functions: A unified framework, benchmark, and new directions. In *2019 IEEE 58th Conference on Decision and Control (CDC)*, pages 238–243. IEEE, 2019.

Peter Wieland and Frank Allgöwer. Constructive safety using control barrier functions. *IFAC Proceedings Volumes*, 40(12):462–467, 2007.

Jingzhao Zhang, Tianxing He, Suvrit Sra, and Ali Jadbabaie. Why gradient clipping accelerates training: A theoretical justification for adaptivity. *arXiv preprint arXiv:1905.11881*, 2019.

Appendix A. Equivalent Loss Function in Problem Formulation

Solving problem (2) is hard since it has infinite number of safety constraints considering that \mathcal{S} is a continuous space. Ma et al. adopts the Lagrangian-based approach. As each state has a safety constraint, each state has a corresponding multiplier denoted by the mapping $\lambda : \mathcal{S} \rightarrow \mathbb{R}$. The mapping can be approximated by a neural network similar to a policy. The corresponding Lagrange function of (2) is

$$\mathcal{L}(\pi, \lambda) = -\mathbb{E}_s v^\pi(s) + \sum_{s \in \mathcal{S}_c} \lambda(s) \left(\phi(s') - \max\{\phi(s) - \eta_D, 0\} \right) \quad (14)$$

However, the sum over state in (14) is unavailable considering the continuity of state space. An alternative Lagrange function is formulated to solve the problem:

$$\mathcal{L}'(\pi, \lambda) = \mathbb{E}_s \left\{ -v^\pi(s) + \lambda(s) \left(\phi(s') - \max\{\phi(s) - \eta_D, 0\} \right) \right\} \quad (15)$$

Equivalence between (14) and (15) can be explained by regarding (3) as one with the reshaped constraints

$$d_\gamma(s) \left(\phi(s') - \max\{\phi(s) - \eta_D, 0\} \right) \leq 0 \quad (16)$$

where $d_\gamma(s)$ is the discounted visiting probability. If the state lies in \mathcal{S}_c , $d_\gamma(s) > 0$ and the constraint (16) is equal to the original constraint (16). Otherwise, $d_i(s) = 0$ which means the safety constraint with respect to those states outside the state set we are interested is not considered. $\mathcal{L}'(\pi, \lambda)$ is a computable loss function in RL, and we can finally solve (2) by locating the saddle point of $\mathcal{L}'(\pi, \lambda)$:

$$\max_{\lambda} \min_{\pi} \mathcal{L}'(\pi, \lambda) \quad (17)$$

Appendix B. Theoretical Results in Section: Joint Synthesis of Safety Certificate and Safe Control Policy

B.1. Proof of Lemma 3

The first part of $\mathcal{L}'(\pi^*, \lambda^*, \phi)$, $-v^\pi(s)$ is irrelevant with ϕ , so we get $\Delta = \mathbb{E}_s \{-v^{\pi^*}(s)\}$. For feasible states $s \in \mathcal{S}_f$ with constraint satisfaction, both clipping and multiplying the optimal multiplier enforce the loss term to be zero. As for $s \notin \mathcal{S}_f$ (i.e., $\lambda(s) \left(\phi(s') - \max\{\phi(s) - \eta_D, 0\} \right) \geq 0$), we

know that $\lambda^*(s) \rightarrow \infty$ from Lemma 2. Then $\lambda^*(s)$ is clipped to λ_{\max} . Therefore, the Lagrange function with (3) can be reformulated to

$$\begin{aligned}
 & \mathcal{L}'(\pi^*, \lambda^*, \phi) \\
 &= \mathbb{E}_s \left\{ -v^\pi(s) + \lambda^*(s) (\phi(s') - \max\{\phi(s) - \eta_D, 0\}) \right\} \Big|_{\pi=\pi^*} \\
 &= \mathbb{E}_s \left\{ \lambda^*(s) (\phi(s') - \max\{\phi(s) - \eta_D, 0\}) \right\} \Big|_{\pi=\pi^*} + \Delta \\
 &= \mathbb{E}_{s \notin \mathcal{S}_f} \left\{ \lambda^*(s) (\phi(s') - \max\{\phi(s) - \eta_D, 0\}) \right\} \Big|_{\pi=\pi^*} + \Delta \\
 &= \lambda_{\max} \mathbb{E}_{s \notin \mathcal{S}_f} \left\{ (\phi(s') - \max\{\phi(s) - \eta_D, 0\}) \right\} \Big|_{\pi=\pi^*} + \Delta \\
 &= \lambda_{\max} J(\phi) + \Delta
 \end{aligned}$$

B.2. Proof of Theorem 6

According to Lemma 3, the gradient of ϕ loss (5) *coincides* with the $\partial \mathcal{L}(\pi^*, \lambda^*, \phi) / \partial \phi$. Therefore, according to the parameterized constrained optimization case of the envelope theorem, $\partial \mathcal{L}(\pi^*, \lambda^*, \phi) / \partial \phi = dJ(\phi) / d\phi$.

Appendix C. Theoretical Results in Section: Practical Algorithm using Constrained Reinforcement Learning

C.1. Gradient Computation

The objective function of updating the policy and multipliers are the Lagrange function in (3). Using the framework of maximum entropy RL, the objective function of policy update is:

$$\begin{aligned}
 J_\pi(\theta) = & \mathbb{E}_{s_t \sim \mathcal{B}} \left\{ \mathbb{E}_{a_t \sim \pi_\theta} \left\{ \alpha \log(\pi_\theta(a_t | s_t)) - \right. \right. \\
 & \left. \left. Q_w(s_t, a_t) + \lambda_\xi(s_t) j_c^\pi(s_t, a_t) \right\} \right\}
 \end{aligned} \tag{18}$$

The policy gradient with the reparameterized policy $a_t = f_\theta(\epsilon_t; s_t)$ can be approximated by:

$$\begin{aligned}
 G_\theta &= \hat{\nabla}_\theta J_\pi(\theta) \\
 &= \nabla_\theta \alpha \log(\pi_\theta(a_t | s_t)) + \left(\nabla_{a_t} \alpha \log(\pi_\theta(a_t | s_t)) \right. \\
 &\quad \left. - \nabla_{a_t} (Q_w(s_t, a_t) - \lambda_\xi(s_t) j_c^\pi(s_t, a_t)) \right) \nabla_\theta f_\theta(\epsilon_t; s_t)
 \end{aligned}$$

where $\hat{\nabla}_\theta J_\pi(\theta)$ represents the stochastic gradient with respect to θ , and $j_c^\pi(s_t, a_t) = (\phi(s_{t+1}) - \max\{\phi(s_t) - \eta_D, 0\})$. Neglecting those irrelevant parts, the objective function of updating the multiplier network parameters ξ is

$$J_\lambda(\xi) = \mathbb{E}_{s_t \sim \mathcal{B}} \left\{ \mathbb{E}_{a_t \sim \pi_\theta} \left\{ \lambda_\xi(s_t) (j_c^\pi(s_t, a_t) - d) \right\} \right\}$$

The stochastic gradient is

$$G_\xi = \hat{\nabla} J_\lambda(\xi) = j_c^\pi(s_t, a_t) \nabla_\xi \lambda_\xi(s_t) \tag{19}$$

The objective function of updating the safety index parameters ζ is already discussed, so the gradients for ζ is

$$G_\zeta = \lambda_\zeta(s_t) \nabla_\zeta \Delta \phi^{\pi_\theta}(s_t) \quad (20)$$

where $\Delta \phi^{\pi_\theta}(s_t) = (\phi(s_{t+1}) - \max\{\phi(s_t) - \eta_D, 0\})|_{\pi_\theta}$, we use a different notation from $j_c^\pi(s_t, a_t)$ since we focus on different variables.

C.2. Proof of Theorem 8

Recall the overview of the total convergence proof:

1. First we show that each update of the multi-time scale discrete stochastic approximation algorithm $(\theta_k, \xi_k, \zeta_k)$ converges almost surely, but at different speeds, to the *stationary point* $(\theta^*, \xi^*, \zeta^*)$ of the corresponding continuous time system.
2. By Lyapunov analysis, we show that the continuous time system is locally asymptotically stable at $(\theta^*, \xi^*, \zeta^*)$.
3. We prove that (θ^*, ξ^*) is locally optimal solution, or a local saddle point for the CRL problems with local optimal safety index parameters ζ^* .

First, we introduce the important lemma used for the convergence proof:

Lemma 9 (Convergence of clipped SGD Zhang et al. (2019)) *For a stochastic gradient descent problem of a continuous differentiable and $L_0 - L_1$ smooth (which means $\|\nabla^2 f(x)\| \leq L_0 + L_1 \|\nabla f(x)\|$) loss function $f(x)$ and its stochastic gradient $\hat{\nabla} f(x)$, If these conditions are satisfied*

1. $f(x)$ is lower bounded;
2. There exists $\tau > 0$, such that $\|\nabla \hat{f}(x) - \nabla f(x)\| \leq \tau$ almost surely;

then the update of stochastic gradient descent converges almost surely with finite iteration complexity.

For satisfying the smoothness condition, we add an additional assumption here:

Assumption 4 *All neural network assumption are $L_0 - L_1$ smooth.*

This assumption is more close to empirical case according to Zhang et al. (2019). Then we continue to finish the multi-timescale convergence: **Step 1** Convergence of θ update **Bounded error**. As the random variable G_θ depends on the state-action pair sampled from replay buffer, so in the following derivation it is denoted as $G_\theta(s, a)$. For the SGD using sampled (s_k, a_k) at k^{th} step, the stochastic gradient is denoted by $G_{\theta_k}(s_k, a_k)$. The error term with respect to θ is computed by

$$\delta \theta_k = G_{\theta_k}(s_k, a_k) - \mathbb{E}_{s \sim d_\gamma^{\pi_\theta}} \{ \mathbb{E}_{a \sim \pi_\theta} G_{\theta_k}(s, a) \} \quad (21)$$

Therefore, the error term is bounded by

$$\begin{aligned} & \|\delta \theta_k\|^2 \\ & \leq 2 \|d_\gamma^{\pi_\theta}(s) \pi(a|s)\|_\infty^2 \left(\|G_{\theta_k}(s, a)\|_\infty^2 + |G_{\theta_k}(s_k, a_k)|^2 \right) \\ & \leq 6 \|d_\gamma^{\pi_\theta}(s) \pi(a|s)\|_\infty^2 \|G_{\theta_k}(s, a)\|_\infty^2 \end{aligned} \quad (22)$$

As we assume the state and action are sampled from a closed set and the continuity of neural network, the upper bounded is valid. According to Lemma 9 and invoking Theorem 2 in Chapter 2 of Borkar's book [Borkar \(2009\)](#), the optimization converges to a fixed point θ^* almost surely (for given ξ, ζ).

Stationary point θ^* . Then we show that the fixed point θ^* is a stationary point using Lyapunov analysis. The analysis of the fastest timescale, θ update, is rather easy, but it is helpful for the similar analysis in the next two time scale. According to [Borkar \(2009\)](#), we can regards the stochastic optimization of θ as a stochastic approximation of a dynamic system for given ξ, ζ :

$$\dot{\theta} = -\nabla_{\theta} \mathcal{L}'(\theta, \xi, \zeta) \quad (23)$$

Proposition 10 *consider a Lyapunov function for dynamic system (23):*

$$L_{\xi, \zeta}(\theta) = \mathcal{L}'(\theta, \xi, \zeta) - \mathcal{L}'(\theta^*(\xi, \zeta), \xi, \zeta) \quad (24)$$

where $\theta^*(\xi, \zeta)$ is a local minimum for given ξ, ζ . In order to show that θ^* is a stationary point, we need

$$dL_{\xi, \zeta}(\theta)/dt \leq 0 \quad (25)$$

Proof We have

$$\frac{dL_{\xi, \zeta}(\theta)}{dt} = -\|\nabla_{\theta} \mathcal{L}'(\theta, \xi, \zeta)\|^2 \leq 0 \quad (26)$$

The equality holds only when $\mathcal{L}'(\theta, \xi, \zeta) = 0$.³ ■

Combining the conclusion about convergence, $\{\theta_k\}$ converges almost surely to a local minimum point θ^* for given ξ . **Step 2** Convergence of λ update **Bounded Error**.

$$G_{\xi_k}(s_k, a_k) - \mathbb{E}_s \{ \mathbb{E}_a G_{\xi_k}(s, a) \} \quad (27)$$

includes two parts:

1. $\delta\theta_{\epsilon}$ caused by inaccurate update of θ (θ should converge to $\theta^*(\xi, \zeta)$ in Timescale 1, but to θ_k near $\theta^*(\xi, \zeta)$):

$$\begin{aligned} \delta\theta_{\epsilon} &= \hat{\nabla}_{\xi} \mathcal{L}'(\theta_k, \xi, \zeta) - \hat{\nabla}_{\xi} \mathcal{L}'(\theta^*(\xi, \zeta), \xi, \zeta) \\ &= (Q^{\pi_{\theta_k}}(s_k, a_k) - Q^{\pi_{\theta^*}}(s_k, a_k)) \nabla_{\xi} \lambda_{\xi}(s_k) \\ &= (\nabla_a Q(s_k, a_k) \nabla_{\theta} \pi(s_k) \epsilon_{\theta_k} + o(\|\epsilon_{\theta_k}\|)) \nabla_{\xi} \lambda_{\xi}(s_k) \end{aligned} \quad (28)$$

Therefore, $\|\delta\theta_{\epsilon}\| \rightarrow 0$ as $\|\epsilon_{\theta}\| \rightarrow 0$. The error is bounded since $\|\epsilon_{\theta}\|$ is a small error, where there must exists a positive scalar ϵ_0 s.t. $\|\epsilon_{\theta}\| \leq \epsilon_0$.

-
3. Similar convergence proof in [Chow et al. \(2017\)](#) assumes that $\theta \in \Theta$ is a compact set, so they spend lots of effort to analyze the case when the θ reaches the boundary of Θ . However, the proposed clipped SGD has released the requirements of compact domain of θ , so the Lyapunov analysis becomes easier for the first timescale.

2. $\delta\xi_k$ caused by estimation error of ξ :

$$\delta\xi_k = G_{\xi_k}(s_k, a_k) - \mathbb{E}_{s \sim d_{\gamma}^{\pi_\theta}} \{ \mathbb{E}_{a \sim \pi_\theta} G_{\xi_k}(s, a) \} \quad (29)$$

$$\begin{aligned} & \|\delta\xi_k\|^2 \\ & \leq 4 \|d_{\gamma}^{\pi_\theta}(s)\pi(a|s)\|_\infty^2 \left(\max \|j_c^\pi(s, a)\|^2 + d^2 \right) \|\nabla_\xi \lambda_\xi(s_t)\|_\infty^2 \end{aligned} \quad (30)$$

Similar to the analysis of Timescale 1 with compact domain of s_k , we can get the valid upper bound.

We again use Lemma 9 and Theorem 2 in Chapter 6 in [Borkar \(2009\)](#) to show that the sequence $\{\xi_k\}$ converges to the solution of following ODE:

$$\dot{\xi} = -\nabla_\xi \mathcal{L}'(\theta^*(\xi, \zeta), \xi, \zeta) \quad (31)$$

Stationary point. Then we show that the fixed point ξ^* is a stationary point using Lyapunov analysis. Note that we have to take ϵ_θ into considerations.

Proposition 11 *For the dynamic system with error term*

$$\dot{\xi} = -\nabla_\xi \mathcal{L}'(\theta^*(\xi, \zeta) + \epsilon_\theta, \xi, \zeta) \quad (32)$$

Define a Lyapunov function to be

$$L_\zeta(\xi) = \mathcal{L}'(\theta^*(\xi, \zeta), \xi, \zeta) - \mathcal{L}'(\theta^*(\xi, \zeta), \xi^*(\zeta), \zeta) \quad (33)$$

where ξ^* is a local maximum point. Then $\frac{dL_\zeta(\xi)}{dt} \leq 0$.

Proof The proof is similar to Proposition 2, only the error of θ should be considered. We prove that the error of θ does not affect the decreasing property here:

$$\begin{aligned} \frac{dL_\zeta(\xi)}{dt} &= -(\nabla_\xi \mathcal{L}'(\theta^*(\xi, \zeta) + \epsilon_\theta, \xi, \zeta))^T \nabla_\xi \mathcal{L}'(\theta^*(\xi, \zeta), \xi, \zeta) \\ &= -\|\nabla_\xi \mathcal{L}'(\theta^*(\xi, \zeta), \xi, \zeta)\|^2 - \delta\theta_\epsilon^T \nabla_\xi \mathcal{L}'(\theta^*(\xi, \zeta), \xi, \zeta) \\ &\leq -\|\nabla_\xi \mathcal{L}'(\theta^*(\xi, \zeta), \xi, \zeta)\|^2 + K_1 \|\epsilon_\theta\| \|\nabla_\xi \mathcal{L}'(\theta^*(\xi, \zeta), \xi, \zeta)\| \end{aligned} \quad (34)$$

where $K_1 = \|\nabla_a Q(s_k, a_k) \nabla_\theta \pi(s_k) \epsilon_{\theta_k}\|_\infty \|\nabla_\xi \lambda_\xi(s_k)\|_\infty \leq \infty$ according to (28) since the compact domain of s_k, a_k according to Assumption 2. As θ converges much faster than ξ according to the multiple timescale convergence in [Borkar \(2009\)](#), we get $dL_\zeta(\xi)/dt \leq 0$. Therefore, there exists trajectory $\xi(t)$ converges to ξ^* if initial state ξ_0 starts from a ball \mathcal{B}_{ξ^*} around ξ^* according to the asymptotically stable systems. ■

Local saddle point of (θ^*, ξ^*) . One side of the saddle point, $\mathcal{L}'(\theta^*(\xi, \zeta), \xi^*(\zeta), \zeta) \leq \mathcal{L}'(\theta, \xi^*(\zeta), \zeta)$ are already provided in previous, so we need to prove here $\mathcal{L}'(\theta^*(\xi, \zeta), \xi^*(\zeta), \zeta) \geq \mathcal{L}'(\theta^*(\xi, \zeta), \xi, \zeta)$. To complete the proof we need that

$$j_c^\pi(s, a) \leq d \text{ and } \lambda^*(s)(j_c^\pi(s, a) - d) = 0 \quad (35)$$

for all s in \mathcal{S}_f , and a sampled from $\pi_{\theta^*}(\xi, \zeta)$. Recall that λ^* is a local maximum point, we have

$$\nabla_{\xi} \mathcal{L}'(\theta^*(\xi, \zeta), \xi^*(\zeta), \zeta) = 0 \quad (36)$$

Assume there exists s_t and action a_t sampled from $\pi^*(s_t)$ so that $j_c^\pi(s_t, a_t) > 0$. Then for λ^* we have

$$\nabla_{\xi} \mathcal{L}'(\theta^*(\xi, \zeta), \xi^*(\zeta), \zeta) = d_{\gamma}^{\pi_{\theta^*}}(s_t) j_c^\pi(s_t, a_t) \nabla_{\xi} \lambda_{\xi}(s_t) \neq 0 \quad (37)$$

The second part only requires that $\lambda^*(s_t) = 0$ when $j_c^\pi(s_t, a_t) < 0$. Similarly, we assume that there exists s_t and ξ^* where $\lambda_{\xi^*}(s_t) > 0$ and $j_c^\pi(s_t, a_t) < d$. there must exists a ξ_0 subject to

$$\xi_0 = \xi^* + \eta_0 d_{\gamma}^{\pi_{\theta^*}}(s_t) (j_c^\pi(s_t, a_t) - d) \nabla_{\xi} \lambda_{\xi}(s_t) \quad (38)$$

for any $\eta \in (0, \eta_0]$ where $\eta_0 \geq 0$. It contradicts the statement the local maximum ξ^* . Then we get

$$\begin{aligned} & \mathcal{L}'(\theta^*(\xi, \zeta), \xi^*(\zeta), \zeta) \\ &= J_r(\theta^*) + \mathbb{E}_{s \sim d_{\gamma}} \{ \lambda_{\xi^*}(s) \mathbb{E}_{a \sim \pi} \{ j_c^\pi(s, a) \} \} = J_r(\theta^*) \\ &\geq J_r(\theta^*) + \mathbb{E}_{s \sim d_{\gamma}} \{ \lambda_{\xi}(s) \mathbb{E}_{a \sim \pi} \{ j_c^\pi(s, a) \} \} \\ &= \mathcal{L}'(\theta^*(\xi, \zeta), \xi, \zeta) \end{aligned} \quad (39)$$

So (θ^*, ξ^*) is a locally saddle point for given safety index parameters ζ . **Step 3** Convergence of ζ update **Bounded error**. Similar to Timescale 2, the error of ζ update includes two parts

1. $\delta\theta_{\epsilon} + \delta\xi_{\epsilon}$ caused by inaccurate update of θ, ξ :

$$\begin{aligned} & \delta\theta_{\epsilon} + \delta\xi_{\epsilon} \\ &= \lambda_{\xi_k}(s_k) \nabla_{\xi} \Delta \phi^{\pi_{\theta_k}}(s_k) - \lambda_{\xi^*}(s_k) \nabla_{\xi} \Delta \phi^{\pi_{\theta^*}}(s_k) \\ &= \lambda_{\xi_k}(s_k) \nabla_{\zeta} \Delta \phi^{\pi_{\theta_k}}(s_k) - \lambda_{\xi_k}(s_k) \nabla_{\zeta} \Delta \phi^{\pi_{\theta^*}}(s_k) \\ &\quad + \lambda_{\xi_k}(s_k) \nabla_{\zeta} \Delta \phi^{\pi_{\theta^*}}(s_k) - \lambda_{\xi^*}(s_k) \nabla_{\zeta} \Delta \phi^{\pi_{\theta^*}}(s_k) \\ &= (\lambda_{\xi_k}(s_k) - \lambda_{\xi^*}(s_k)) \nabla_{\zeta} \Delta \phi^{\pi_{\theta^*}}(s_k) \end{aligned} \quad (40)$$

The first part after the second equal sign is neglected since θ permutation has no effect on gradient of ζ . Similar to derivation in (28), we get $|\delta\theta_{\epsilon} + \delta\xi_{\epsilon}| \rightarrow 0$ as $(\theta, \xi) \rightarrow (\theta^*, \xi^*)$.

2. $\delta\zeta_k$ caused by estimation error of ζ :

$$\delta\zeta_k = \lambda_{\xi^*}(s_k) \nabla_{\zeta} \Delta \phi^{\pi_{\theta^*}}(s_k) - \mathbb{E} \{ \lambda_{\xi^*}(s) \nabla_{\zeta} \Delta \phi^{\pi_{\theta^*}}(s) \} \quad (41)$$

The bounded error can be obtained by

$$\begin{aligned} & \|\delta\zeta_k\|^2 \\ &\leq 4 \left\| d_{\gamma}^{\pi_{\theta}}(s) \pi(a|s) \right\|_{\infty}^2 \max_{s \in \mathcal{U}_{\mathcal{S}_c} \mathcal{S}_f} |\lambda_{\xi^*}(s)|^2 \|\nabla_{\zeta} \Delta \phi^{\pi_{\theta^*}}(s)\|^2 \end{aligned} \quad (42)$$

Therefore, the ζ -update is a stochastic approximation of the continuous system $\zeta(t)$, described by the ODE For the dynamic system

$$\dot{\zeta} = -\nabla_{\zeta} \mathcal{L}'(\theta, \xi, \zeta)|_{\theta=\theta^*(\xi, \zeta)+\epsilon_{\theta}, \xi=\xi^*(\zeta)+\epsilon_{\xi}} \quad (43)$$

Algorithm 2 FAC-SIS**Input:** $w_1, w_2, w_C, \theta, \xi$.

```

1: Initial target network parameters and buffer
2: for each iteration do
3:   for each environment step do
4:      $a_t \sim \pi_\theta(a_t|s_t), s_{t+1} \sim p(s_{t+1}|s_t, a_t)$ 
5:     Compute  $c(s_t, a_t)$ 
6:      $\mathcal{B} \leftarrow \mathcal{B} \cup \{(s_t, a_t, r(s_t, a_t), c(s_t, a_t), \phi(s_t), s_{t+1})\}$ 
7:   end for
8:   for each gradient step do
9:      $w_i \leftarrow w - \beta_Q G_{w_i}$  for  $i \in \{1, 2\}$ 
10:    if gradient steps mod  $m_\pi = 0$  then  $\theta \leftarrow \theta - \overline{\beta_\pi} G_\theta, \alpha \leftarrow \alpha - \overline{\beta_\alpha} G_\alpha$ 
11:    if gradient steps mod  $m_\lambda = 0$  then  $\xi \leftarrow \xi + \overline{\beta_\lambda} G_\xi$ 
12:    if gradient steps mod  $m_\phi = 0$  then  $\zeta \leftarrow \zeta - \overline{\beta_\zeta} G_\zeta$ 
13:    Update target network.
14:  end for
15: end for

```

Output: w_1, w_2, θ, ξ .**Stationary point.** Define a Lyapunov function

$$L(\zeta) = \mathcal{L}'(\theta^*(\xi, \zeta), \xi^*(\zeta), \zeta) - \mathcal{L}'(\theta^*, \xi^*, \zeta^*) \quad (44)$$

where $\zeta^* \in Z$ is a local minimum point. Then

$$\begin{aligned}
& \frac{dL(\zeta)}{dt} \\
&= (-\nabla_\zeta \mathcal{L}'(\theta^*(\xi, \zeta) + \epsilon_\theta, \xi^*(\zeta) + \epsilon_\xi, \zeta))^T \nabla_\zeta \mathcal{L}'(\theta^*(\xi, \zeta), \xi^*(\zeta), \zeta) \\
&\leq -\|\nabla_\zeta \mathcal{L}'(\theta^*(\xi, \zeta), \xi^*(\zeta), \zeta)\|^2 \\
&\quad + K_2 \|\epsilon_\xi\| \|\nabla_\zeta \mathcal{L}'(\theta^*(\xi, \zeta), \xi^*(\zeta), \zeta)\|
\end{aligned} \quad (45)$$

where $K_2 = \|\nabla_\xi \lambda_\xi(s)\|_\infty \|\nabla_\zeta \Delta \phi^{\pi_{\theta^*}}(s)\|_\infty$ according to (40). The derivation is very simialar to the conclusion in Proposition 11, the upper bound is valid since the compact domain of state and action. As ξ converges faster than ζ , $dL_\zeta(\xi)/dt \leq 0$, so there exists trajectory $\xi(t)$ converges to ξ^* if initial state ζ_0 starts from a ball \mathcal{B}_{ζ^*} around ζ^* according to the asymptotically stable systems.

Finally, we can come to the conclusion that the sequence $(\theta_k, \xi_k, \zeta_k)$, will converge to a locally optimal policy and multiplier tuple (θ^*, ξ^*) for a locally optimal safety index parameters, ζ^* .

Appendix D. Implementation Details**D.1. Algorithm details****D.2. Codebase and Platforms**

Implementation of FAC-SIS, FAC with ϕ_h and ϕ_F are based on the Parallel Asynchronous Buffer-Actor-Learner (PABAL) architecture proposed by Duan et al. (2021). All experiments are imple-

Algorithm 3 FAC with ϕ_h and ϕ_F **Input:** $w_1, w_2, w_C, \theta, \xi$.

```

1: Initial target network parameters and buffer
2: for each iteration do
3:   for each environment step do
4:     Sample and compute cost with (??) using different safety index parameters with respect to
        $\phi_h$  or  $\phi_F$ .
5:     Store transitions  $(s, a, r, c, s')$  to replay buffer.
6:   end for
7:   for each gradient step do
8:      $w_i \leftarrow w - \beta_Q G_{w_i}$  for  $i \in \{1, 2\}$ 
9:     if gradient steps mod  $m_\pi = 0$  then
10:       $\theta \leftarrow \theta - \beta_\pi G_\theta$ 
11:       $\alpha \leftarrow \alpha - \beta_\alpha G_\alpha$ 
12:    end if
13:    if gradient steps mod  $m_\lambda = 0$  then
14:       $\xi \leftarrow \xi + \beta_\lambda G_\xi$ 
15:    end if
16:    Update target network.
17:  end for
18: end for

```

Output: w_1, w_2, θ, ξ .

mented on Intel Xeon Gold 6248 processors with 12 parallel actors, including 4 workers to sample, 4 buffers to store data and 4 learners to compute gradients. Implementation of other baseline algorithms are based on the code released by Ray et al. (2019)⁴ and also a modified version of PPO⁵. We set a different update interval schedule to better adapt to the multiple timescale design and the practical convergence performance in Algorithm 2, which is common in adversarial training.

D.3. Baseline Algorithms

The pseudocode for baseline algorithm, FAC with ϕ_h , ϕ_F , in experiment section are shown in Algorithm 3.

Appendix E. Hyperparameters

The neural network design and detailed hyperparameters are listed in Table 2.

Appendix F. Additional Experimental Results**F.1. Experiments in Other Safety Gym environments**

We select 6 different Safety Gym environments and results of 4 of them are listed in the experiment section. The results with the rest of environments are demonstrated here:

4. <https://github.com/openai/safety-starter-agents>

5. <https://github.com/ikostrikov/pytorch-a2c-ppo-acktr-gail>

The results in the other two environments are consistent with the results in the experiment section. The propose FAC-SIS learns a safe policy with zero constraint violation, and other baseline algorithms all fail to neglect the cost even in the converged policy. Furthermore, the reward performance is better than the handcrafted safety index, or FAC with ϕ_h .

F.2. Custom Environment Details

The custom environment in Figure 6 includes a static goal point at $(0, 5)$, a hazard with radius of 0.5, and a point agent with 2 inputs, rotation and acceleration, the arrow represents the positive direction of the acceleration. The random initial position (including position, heading angle of the agent and the position of hazard) design of three different distributions are listed in Table 1. The reward design includes two parts that are the tracking error of the heading angle towards goal position, and speed relevant to the distance to the goal position (It requires that the agent always takes 5 seconds to reach the goal, so the closer the agent get to the goal, the slower its target speed is.).

Distribution	Agent Initial Position		
Index	x	y	Angle
1	0	$[-1.5, -1.0]$	$[-\pi/4, \pi/4]$
2	0	$[-1.5, -0.5]$	$[-\pi/4, \pi/4]$
3	$[-0.5, 0.5]$	$[-1.5, -0.5]$	$[-\pi/4, \pi/4]$

Distribution	Hazard Initial Position	
Index	x	y
1	0	$[0.5, 1]$
2	0	$[0.5, 1.5]$
3	0	$[0.5, 1]$

Table 1: Initial distribution in custom environments. The initial position is sampled with a uniform distribution between the interval in the table.

Algorithm	Value
<i>FAC-SIS, FAC w/ ϕ_h, FAC w/ ϕ_F</i>	
Optimizer	Adam ($\beta_1 = 0.9, \beta_2 = 0.999$)
Approximation function	Multi-layer Perceptron
Number of hidden layers	2
Number of hidden units per layer	256
Nonlinearity of hidden layer	ELU
Nonlinearity of output layer	linear
Actor learning rate	Linear annealing $3e-5 \rightarrow 1e-6$
Critic learning rate	Linear annealing $8e-5 \rightarrow 1e-6$
Learning rate of multiplier net	Linear annealing $5e-6 \rightarrow 5e-6$
Learning rate of α	Linear annealing $8e-5 \rightarrow 8e-6$
Learning rate of safety index parameters (FAC-SIS only)	Linear annealing $8e-6 \rightarrow 1e-6$
Reward discount factor (γ)	0.99
Policy update interval (m_π)	3
Multiplier ascent interval (m_λ)	12
SIS interval (m_ϕ)	24
Target smoothing coefficient (τ)	0.005
Max episode length (N)	
Safety Gym task	1000
Custom task	120
Expected entropy ($\overline{\mathcal{H}}$)	$\overline{\mathcal{H}} = -\text{Action Dimentions}$
Replay buffer size	5×10^5
Replay batch size	256
Handcrafted safety index (ϕ_h) hyperparameters (η, n, k, σ)	(0, 2, 1, 0.3)
Feasible safety index (ϕ_F) hyperparameters (η, n, k, σ)	(0, 2, 1, 0.04)
<i>CPO, TRPO-Lagrangian</i>	
Max KL divergence	0.1
Damping coefficient	0.1
Backtrack coefficient	0.8
Backtrack iterations	10
Iteration for training values	80
Init λ	$0.268(\text{softplus}(0))$
GAE parameters	0.95
Batch size	2048
Max conjugate gradient iterations	10
<i>PPO-Lagrangian</i>	
Clip ratio	0.2
KL margin	1.2
Mini Bactch Size	64

Table 2: Detailed hyperparameters.

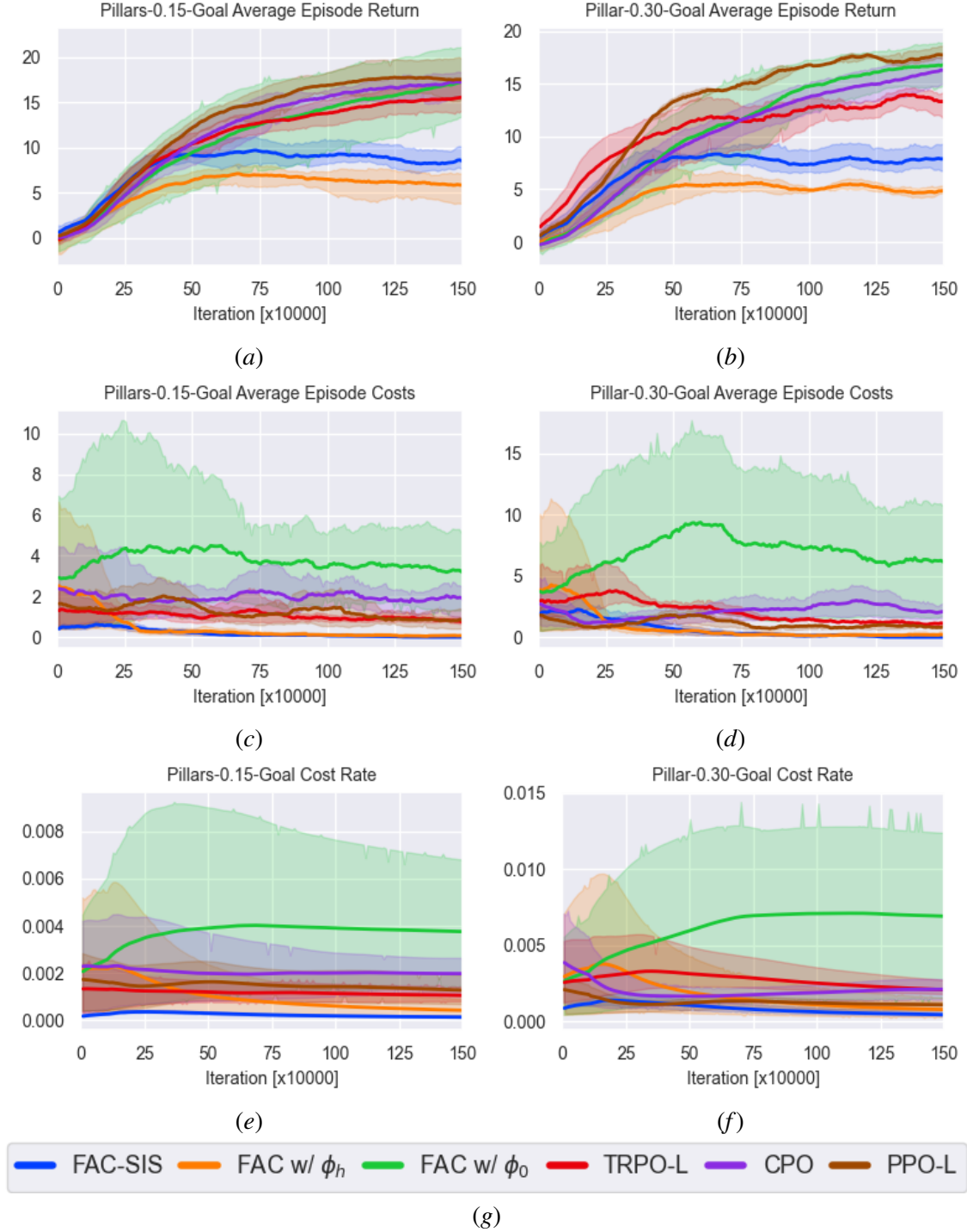


Figure 5: Average performance of FAC-SIS and baseline methods on 2 additional Safety Gym environments over five seeds.

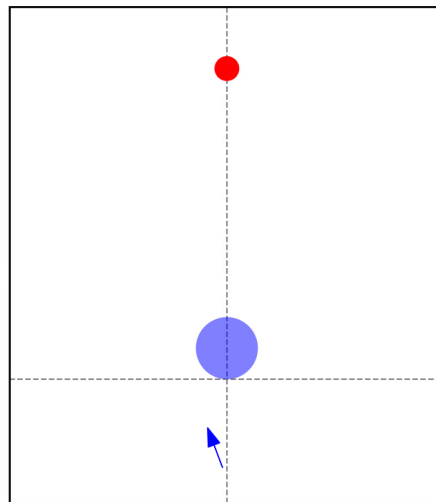


Figure 6: Custom environments.